

PCCP

Accepted Manuscript

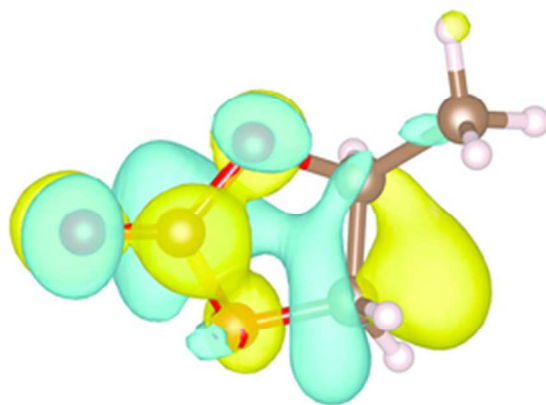


This is an *Accepted Manuscript*, which has been through the Royal Society of Chemistry peer review process and has been accepted for publication.

Accepted Manuscripts are published online shortly after acceptance, before technical editing, formatting and proof reading. Using this free service, authors can make their results available to the community, in citable form, before we publish the edited article. We will replace this *Accepted Manuscript* with the edited and formatted *Advance Article* as soon as it is available.

You can find more information about *Accepted Manuscripts* in the [Information for Authors](#).

Please note that technical editing may introduce minor changes to the text and/or graphics, which may alter content. The journal's standard [Terms & Conditions](#) and the [Ethical guidelines](#) still apply. In no event shall the Royal Society of Chemistry be held responsible for any errors or omissions in this *Accepted Manuscript* or any consequences arising from the use of any information it contains.



X-Ray absorption spectra, interpreted using first-principles electronic structure calculations, provide insight into the solvation of the lithium ion in propylene carbonate.
38x19mm (300 x 300 DPI)

X-Ray Absorption Spectroscopy of LiBF_4 in Propylene Carbonate: A Model Lithium Ion Battery Electrolyte

Jacob W. Smith,^{a,b} Royce K. Lam,^{a,b} Alex T. Sheardy,^{a,b} Orion Shih,^a Anthony M. Rizzuto,^a Oleg Borodin,^c Stephen J. Harris,^d David Prendergast,^e and Richard J. Saykally^{a,b,*}

a. Department of Chemistry, University of California, Berkeley, California 94720, USA

b. Chemical Sciences Division, Lawrence Berkeley National Laboratory, Berkeley, California 94720, USA

c. Electrochemistry Branch, U.S. Army Research Laboratory, Adelphi, Maryland 20783, USA

d. Materials Sciences Division, Lawrence Berkeley National Laboratory, Berkeley, California 94720, USA

e. Molecular Foundry, Lawrence Berkeley National Laboratory, Berkeley, California 94720, USA

** To whom correspondence should be addressed*

ABSTRACT

Since their introduction into the commercial marketplace in 1991, lithium ion batteries have become increasingly ubiquitous in portable technology. Nevertheless, improvements to existing battery technology are necessary to expand their utility for larger-scale applications, such as electric vehicles. Advances may be realized from improvements to the liquid electrolyte; however, current understanding of the liquid structure and properties remain incomplete. X-ray absorption spectroscopy of solutions of LiBF_4 in propylene carbonate (PC), interpreted using first-principles electronic structure calculations within the eXcited electron and Core Hole (XCH) approximation, yields new insight into the solvation structure of the Li^+ ion in this model electrolyte. By generating linear combinations of the computed spectra of Li^+ -associating and free PC molecules and comparing to the experimental spectrum, we find a Li^+ -solvent interaction number of 4.5. This result suggests that computational models of lithium ion battery electrolytes should move beyond tetrahedral coordination structures.

INTRODUCTION

Lithium ion batteries (LIBs) have rapidly grown to dominate the rechargeable battery market for portable technology. Given the simultaneous expansion of the market for handheld devices (i.e. cellular phones, laptops, tablets, etc.), LIBs now comprise a multibillion dollar industry.¹ Such demand has spurred intense research and development efforts.² Nevertheless, serious shortcomings persist which limit the utility of modern LIBs for larger-scale applications in electric vehicles (EVs) or for power storage utilized in conjunction with intermittent renewable energy sources (wind, solar, etc.).²⁻⁴ These shortcomings include high cost, energy density below optimal EV standards, slow recharging rates, and limited lifetimes.

A typical commercial LIB consists of a graphite negative electrode and metal oxide or metal phosphate positive electrode (e.g. LiCoO_2 , LiFePO_4 , LiMnO_2 , etc.). Charge is transported by lithium ions travelling between the electrodes through a liquid electrolyte commonly consisting of a lithium salt with a large, charge-disperse anion such as PF_6^- , BF_4^- , ClO_4^- , or more recently larger, carbon-based anions such as bis(oxalato)borate $\{\text{B}(\text{C}_2\text{O}_4)_2\}^-$; BOB $\}$ dissolved in a non-aqueous solvent. These solvents typically consist of combinations of linear alkyl carbonate molecules such as dimethyl carbonate (DMC) and ethyl methyl carbonate (EMC), and the cyclic alkyl carbonate ethylene carbonate (EC). Propylene carbonate (PC), a structural analogue of EC with a methyl group on a ring carbon, is unsuitable for use in commercial batteries, as it penetrates and ultimately damages the graphite electrode. Oxidation and reduction of the liquid electrolyte at the electrodes during initial cycling results in the formation of the “solid-electrolyte interphase (SEI),”^{5–9} consuming liquid electrolyte and incorporating some of the Li^+ charge carriers from the cell. This passivating layer is thought to grow until it has become sufficiently resistive to fully restrict electron transfer between the electrode and liquid electrolyte while allowing passage of Li^+ .³ Thereafter, minimal damage occurs in the liquid electrolyte.

A great deal of effort has been dedicated to investigation of the electrodes and associated SEI of LIBs and the transport of Li^+ through these media.^{2,5,6,10–14} Substantially less study has been directed towards the liquid electrolyte.¹⁵ It is becoming increasingly clear, however, that the structure of the liquid electrolyte substantially influences the function of LIBs, and that improvements to the liquid electrolyte are an essential component of the overall effort to improve LIBs for use in EVs and large-scale energy storage. Several studies have demonstrated that the solvation environment of the lithium ion in the electrolyte dictates the formation mechanism and resulting structure of the SEI.^{7,16–18} This is significant for a number of reasons: SEI growth consumes Li^+ , produces a high-resistivity region through which ions must migrate, and is widely implicated as the region of the battery in which failure is most likely to occur.¹⁹ Furthermore, recent studies by Xu *et al.* have suggested that the desolvation of the Li^+ from the liquid electrolyte is the slow step in Li^+ insertion into the electrodes, thus comprising a critical limitation on power density and recharging rates.^{20,21} Clearly, improvements in the electrolytic properties will improve nearly all significant aspects of LIB performance, including energy and power density, recharge time, and cycle life.

In order to realize the performance enhancements from improved electrolytes, it is necessary to thoroughly understand the electrolyte structure. Unfortunately, while a number of studies have been performed on LIB electrolyte systems, a clear picture of the solvation structure of the Li^+ ion in alkyl carbonate solutions remains elusive. For example, several experimental and theoretical studies have suggested that a substantial degree of ion pairing/aggregation exists between Li^+ and the counterion (BF_4^- , ClO_4^- , PF_6^-) at concentrations of $\sim 1\text{M}$ (1 mol/dm^3), the approximate solution concentration in standard commercial LIBs.^{22–25} Other studies of the electrochemical properties and infrared and Raman spectra of the same solutions and concentrations have suggested little or no ion pairing or aggregation.^{16,26,27} Similarly, the interactions of the ions with the solvent remain incompletely characterized. The generally favored structure comprises a tetrahedral coordination of carbonyl oxygen atoms around the Li^+ and weakly solvated counterions. Numerous experimental and theoretical studies have found total coordination numbers for Li^+ (Li-O + Li-counterion interactions) very near four.^{8,25,28,29} However, several vibrational spectroscopy studies (infrared absorption, Raman) of LIB electrolytes have suggested Li^+ coordination numbers between 4 and 5.^{16,30,31} A study published by Kondo *et al.* utilized conductivity measurements to estimate the coordination number of Li^+ in PC at 4.3.²⁷ Neutron diffraction studies by Kameda *et al.* have found a Li-O coordination number of 4.5 in the same electrolyte solution.³² Bogle *et al.* have interpreted the chemical shifts in ^{17}C NMR to ascertain a Li-O coordination number of 5.69 for LiPF_6 in EC,³³ while at least one study utilizing NMR diffusivity measurements has estimated a coordination number for Li^+ as LiClO_4 in EC to be ~ 7 in concentrations up to $\sim 1\text{M}$.³⁴

Here we investigate the coordination structure of Li^+ in solutions of LiBF_4 in PC using x-ray absorption spectroscopy (XAS) of liquid microjets.³⁵ XAS is an atom-specific core-level spectroscopic probe of the unoccupied electronic states; as such, it is sensitive to both the intra- and intermolecular environment of the target atom. Experimental spectra are interpreted through utilization of molecular dynamics simulations and spectral simulations computed using the Prendergast-Galli eXcited electron and Core Hole (XCH) methodology.³⁶ Previous studies in our group have used these experimental and theoretical techniques to investigate the structure and chemistry of a variety of aqueous solutions.^{37–40} Here, we extend the methodology to a non-aqueous system of substantial practical utility for the purpose

of understanding and improving the solvation properties and desolvation process of the Li^+ ion in LIB electrolytes.

EXPERIMENTAL AND THEORETICAL METHODS

a. X-ray spectroscopy of liquid microjets

LiBF_4 and PC were obtained from Sigma Aldrich and had minimum purity of 98% and 99.7%, respectively. PC was stored under dry nitrogen until use. X-ray absorption spectra were collected at Beamline 8.0.1 of the Advanced Light Source at Lawrence Berkeley National Laboratory (Berkeley, CA); this beamline has a nominal maximum output of 6×10^{15} photons/s with resolving power $E/\Delta E$ of 7000. Liquid jets are produced by forcing pressurized (~ 15 bar) liquids through a $100 \mu\text{m}$ inner diameter silica capillary into a vacuum chamber (10^{-5} torr), where they interact with the x-ray beamline. Total electron yield (TEY) XA spectra are collected on a 2.1 kV biased copper as a function of photon energy. Our previous work has demonstrated that spectra obtained in this manner are representative of the bulk liquid.^{41,42} Spectra are normalized to the signal collected simultaneously on a high-transmission gold grid intersecting the beamline several meters before it is focused into the chamber. Unlike previous work published by our group, this paper presents liquid spectra without gas-phase background subtraction; the low vapor pressure of PC (< 2 torr at 298K) renders the gas phase spectrum insignificant, accounting for $< 0.2\%$ of total intensity. Full XA spectra of the carbon and oxygen K-edges were collected with 0.2 eV step sizes and 1s count times; detailed spectra of the oxygen K-edge were collected with 0.05 eV steps and 2s count times. Single-point energy axis calibrations were performed using gas-phase carbon dioxide for the carbon K-edge and liquid water for the oxygen K-edge. A more complete description of the experiment can be found in a prior publication.³⁵

b. Molecular dynamics simulations

A many-body polarizable force field (FF) APPLE&P⁴³ (Atomistic Polarizable Potential for Liquids, Electrolytes, and Polymers) has been used for molecular dynamics (MD) simulations of PC and (PC) LiBF_4 electrolytes. APPLE&P utilizes an exp-6 form for description of non-bonded interactions, also called the Buckingham potential, in conjunction with permanent charges situated on atomic sites and off-ether oxygen atomic sites for PC. The many-body polarization interactions are represented by the induced isotropic atomic dipoles and were solved self-consistently. The short-range interaction between

induced dipoles is screened using Thole methodology with the Thole parameter ($a_T=0.4$). Atoms connected by bonds (1-2) and bends (1-2-3) were excluded from the list of non-bonded interactions. Atoms connected by 3 or more bonds had full non-bonded interactions with the exception that 1-4 interaction between permanent charges and induced dipoles were scaled by 0.8. A detailed discussion of the functional form is provided elsewhere.⁴³ Previously developed PC and PC/Li⁺ force field parameters were used.^{44,45} APPLE&P parameters⁴⁶ for LiBF₄ were modified by refitting BF₄⁻ charges to electrostatic potential around anion obtained at MP2/aug-cc-pvTz level, while Li...F repulsion parameters were refit to Li⁺/BF₄⁻ binding energy obtained at the same level. The revised force field version was denoted as "e44." The revised force field yielded ion self-diffusion coefficients and ionic conductivity of PC/LiBF₄ electrolytes in excellent agreement with experiments (available in Supplemental Information).

We closely followed the simulation methodology previously used in MD simulations of electrolytes containing lithium salts.^{45,46} Two PC-LiBF₄ systems have been constructed: a *large* simulation cell containing 640 PC and 64 LiBF₄, and a *small* simulation cell containing 20 PC and 2 LiBF₄. Simulations were performed at 298 K. Equilibration runs were 6 ns at 333 K followed by 3 ns and 6 ns equilibration runs in NPT ensemble at 298 K for the large and small systems, respectively. The density of the large box was imposed upon the small box to compensate for large density fluctuations arising from the small sample size. Production runs were performed for 8.3 ns and 1 ns for the large and small systems, respectively, in the NVT ensemble. The cutoff for non-bonded interactions was set to 12 Å for the large box and at half a box for the small simulation cell. Snapshots of the molecular configurations of the small simulation box were saved at 20 ps intervals for the spectral simulations. Snapshots from a small box containing 20 PC were generated following the same methods.

c. Spectral Simulations

Simulated spectra of the oxygen K-edge of PC and the (PC)LiBF₄ electrolyte were calculated using the XCH approximation,³⁶ a first-principles constrained-occupancy density functional theory (DFT) calculation, using molecular coordinates sampled from the small box MD simulations described above. DFT calculations were performed under periodic boundary conditions using the Plane Wave Self-Consistent Field (PWSCF) program within the Quantum-ESPRESSO package,⁴⁷ employing the Perdew-Burke-Ernzerhof form of the Generalized Gradient Approximation to the exchange-correlation potential.⁴⁸

The plane wave basis set, with a 25 Ry kinetic energy cutoff, is sufficiently flexible to model both localized and delocalized Kohn-Sham orbitals in the XCH approximation to the core-excited states. The electron density of the lowest energy core-excited state was generated self-consistently with explicit inclusion of a core hole on a target oxygen atom, modeled with a suitably modified pseudopotential, together with the inclusion of the excited electron in the first available valence orbital. Higher energy excited states were approximated using the unoccupied Kohn-Sham orbitals of the XCH self-consistent field. Transition matrix elements were computed within Fermi's Golden Rule between the 1s atomic orbital of the ground state and the unoccupied orbitals from the XCH calculation. Resulting transitions were broadened via Gaussian convolution using a fixed linewidth parameter of 0.2 eV to produce the final simulated spectrum. Spectra obtained from independent excited atoms and/or MD snapshots were aligned based on an isolated atomic reference, utilizing a previously-published methodology,³⁹ using the spectrum of gaseous CO₂ to provide a single-point energy alignment to experiment.

RESULTS AND DISCUSSION

a. XAS of PC and (PC)LiBF₄

The TEY XA spectra collected for the carbon and oxygen K-edges of neat PC and 1M LiBF₄ in PC are shown in Figures 1 and 2, respectively. As the carbon K-edge spectrum exhibits no significant changes upon addition of the lithium salt, no additional analysis has been performed for these spectra. However, several features in the oxygen K-edge spectrum exhibit a blue shift in the (PC)LiBF₄ electrolyte relative to the analogous features in the spectrum of the neat solvent. Detailed spectra on the first sharp feature in the oxygen K-edge spectra, near 533.5 eV, were collected for neat PC and solutions of 0.25, 0.5, and 1.0 M LiBF₄ in PC (Figure 3). This feature exhibits a progressive blue shift, increasing as a function of LiBF₄ concentration, with a total shift of 0.07 eV from neat PC to the 1M solution. As this spectral feature is much sharper and more clearly defined than those near 538 and 543 eV, which also exhibit blue shifts upon addition of the lithium salt, we have chosen to focus our analysis on this region of the spectrum.

b. MD simulations

The large-box MD simulations produced values for diffusivity, conductivity, and degree of uncorrelated ionic motion (iconicity) in excellent agreement with previously reported experimental

values;²⁵ these values are tabulated in the Supplemental Information. A comparison of the structural parameters of the small and large boxes is presented in Figure 4, with additional parameters found in the Supplemental Information. The small box does exhibit a small increase in ion aggregation (Li..F association number of 1.95 for the large box, 2.1 for the small box), likely facilitated by the enforced proximity of ions in the small box. The increase in Li⁺..BF₄⁻ association is balanced by a corresponding decrease in the number of Li⁺-solvent interactions in the first solvation shell (2.3 large box, 2.15 small box), resulting in a constant value for the total lithium coordination number (~4.25). The Li⁺..carbonyl interaction lengths and Li⁺..O=C angular distributions are very similar for the small and large boxes (average Li⁺..O=C angle 149.2° large box, 148.4° small box). This suggests that the interactions between the lithium ion and solvent molecules are not substantially altered by the small system size in the small simulation box.

c. Spectral simulations

Due to the high computational cost of performing first-principles electronic structure calculations on large systems, the XCH calculation was performed using molecular configurations sampled from the small simulation boxes containing 20 PC for the neat liquid and 20 PC with 2 LiBF₄ for the electrolyte. The calculated spectrum of neat PC, shown in the bottom panel of Figure 2, reproduces the experimental spectrum well. The calculated spectrum of the (PC)LiBF₄ electrolyte solution does not exhibit the characteristic blue shift relative to the neat liquid observed in the experimental spectrum. Observed transitions in the XA spectrum were assigned with the assistance of isosurfaces generated for the states comprising each of the four major spectral features in neat PC. These isosurfaces, presented in Figure 5, suggest that the sharp features near 533.5 and 536.5 eV represent transitions to the π-antibonding system from the carbonyl and ring oxygen atoms, respectively. The broader, higher-energy states represent 1s-σ* transitions. As observed in the isosurfaces, the σ* states are highly disperse, with substantial density on neighboring molecules; as such, configurational broadening arising from inhomogeneity of the liquid environment is the primary source of spectral broadening for these features. The π* system is more localized, minimizing inhomogeneous broadening, explaining the narrower spectral width of features associated with transitions into this state. Other significant sources of broadening for these features include core-hole lifetime broadening and vibrational broadening.⁴⁹ In the

condensed phase, vibrational structure is broadened, resulting in asymmetric features weighted towards the blue;⁵⁰ such structure is observed in the π^* features of the experimental spectra. Each σ^* feature contains spectral intensity for transitions originating from both carbonyl and ring oxygen atoms. While the calculated spectrum does not reproduce the experimental blue shift from PC to (PC)LiBF₄, the features in the experimental spectrum exhibiting the shift originate at least in part from the carbonyl oxygen. The largest shift is observed in the carbonyl π^* feature. Less dramatic shifts are observed for the σ^* features, resulting from shifting only of the spectral lines associated with transitions originating from the carbonyl oxygen. The ring 1s to π^* transition exhibits very little shift in the experimental spectrum. These observations support the Raman findings of Kondo *et al*, which suggest that Li⁺-PC interactions at concentrations below 2M occur nearly exclusively at the carbonyl oxygen of PC.²⁷

d. Evaluation of the Li⁺-PC coordination number

We divided the PC molecules in the molecular coordinates utilized to generate the calculated spectrum of PC(LiBF₄) into two groups: those associating directly with the Li⁺ ion (i.e. in the first solvation shell, Li..O=C separation <2.5 Å), and those not directly associating with Li⁺ (free PC). Within the molecular coordinates sampled, no interactions were observed between Li⁺ and PC except via the carbonyl oxygen; i.e. no ring oxygen or carbon atoms were located within the 2.5 Å interaction range. The spectra calculated from excitations from the carbonyl and ring oxygen in the associating and non-associating molecule groups were averaged to produce independent spectra for PC associating with Li⁺ and free PC. These spectra are displayed in Figure 6. As predicted, there is no substantive difference in the spectrum of ring oxygen between associating and non-associating molecules. However, the carbonyl oxygen spectrum of Li⁺-associating PC molecules does exhibit a blue shift relative to that of free PC; for the carbonyl π^* feature centered at 533.5 eV, the peak is shifted by 0.35 eV, substantially greater than the experimental shift of 0.07 eV between the neat liquid and 1M electrolyte solution. Thus, the inability of the initial theoretical calculations to reproduce the experimentally observed blue-shift most likely results from an underestimation of the association number of Li⁺-PC in the MD simulations. In order to estimate the correct association number, we have generated linear combinations of the computed carbonyl oxygen XAS spectra of associating and non-associating carbonyl oxygen for ratios of 20-50% associating molecules. The carbonyl π^* region of these linearly combined spectra are presented in Figure 7, along

with a line indicating the location of the center of the carbonyl $1s-\pi^*$ transition feature in the experimental spectrum of 1M LiBF_4 in PC. The experimental shift is best reproduced by the combination containing 40% ($\pm 2\%$) Li^+ -associating molecules. A comparison of the linear combination for this proportion of Li^+ -associating PC to the experimental spectrum is shown in Figure 8 and exhibits excellent agreement. Using a density of 1M (PC) LiBF_4 of 1.251 kg/dm^3 ,²⁵ this association proportion corresponds to an average Li^+ -PC association number of $4.5 (\pm 0.2)$. While incongruous with the standard tetrahedral model of Li^+ solvation in electrolyte systems,^{8,25,28,29} this value is in excellent agreement with that measured in neutron diffraction experiments³² as well as IR studies of Li^+ -EC.¹⁶

CONCLUSIONS

The oxygen K-edge XA spectrum of PC exhibits a small blue shift upon addition of LiBF_4 which increases as a function of concentration. Shifts are only observed in spectral features associated with transitions from the carbonyl oxygens; transitions from the ring oxygens are unaffected by the addition of salt. XCH calculations have shown that the spectrum of free PC in the electrolyte solution is unchanged from that of the neat liquid, while the spectra of PC molecules coordinating Li^+ exhibit a blue shift. The experimental electrolyte spectrum can be accurately modeled as a linear combination of the spectra of Li^+ -associating and free PC molecules. A linear combination of 40% lithium-associating and 60% free PC best reproduces the experimental spectrum of 1M LiBF_4 . From this ratio we have calculated a $\text{Li}^+ \cdots \text{O}=\text{C}$ association number of 4.5 ± 0.2 . MD simulations developed to provide molecular coordinates for the XCH calculation produced bulk solution properties in good agreement with experimental values. However, on the molecular scale they underestimate the solvation number of Li^+ -PC relative to the experimental value determined in this study. New theoretical investigations of LIB electrolyte solutions allowing for a substantial number of non-tetrahedral Li^+ solvation structures will produce a more accurate model of the real solutions and may provide a route to improvements to current battery technology.

ACKNOWLEDGEMENTS

This work was supported by facilities of the Lawrence Berkeley National Laboratory, the Advanced Light Source and National Energy Research Scientific Computing Center, supported by the Director, Office of Science, Office of Basic Energy Sciences, of the U.S. Department of Energy under Contract No. DE-AC02-05CH11231. The authors would like to acknowledge the excellent experimental support of all staff

at the Advanced Light Source, with special thanks to Wanli Yang, Jonathan Spear, Alejandro Aguilar, and David Kilcoyne.

REFERENCES

1. V. Narain, *Global Industrial Batteries Market*, Report, Frost & Sullivan, 2013.
2. J. B. Goodenough and K.-S. Park, *J. Am. Chem. Soc.*, 2013, **135**, 1167–76.
3. J. B. Goodenough and Y. Kim, *Chem. Mater.*, 2010, **22**, 587–603.
4. M. Armand and J.-M. Tarascon, *Nature*, 2008, **451**, 652–7.
5. D. Aurbach, *J. Power Sources*, 2000, **89**, 206–218.
6. E. Peled, *J. Electrochem. Soc.*, 1997, **144**, L208.
7. P. Ganesh, P. R. C. Kent, and D. Jiang, *J. Phys. Chem. C*, 2012, **116**, 24476–24481.
8. K. Leung and J. L. Budzien, *Phys. Chem. Chem. Phys.*, 2010, **12**, 6583–6.
9. L. Xing, W. Li, C. Wang, F. Gu, M. Xu, C. Tan, and J. Yi, *J. Phys. Chem. B*, 2009, **113**, 16596–602.
10. J. B. Goodenough, *Acc. Chem. Res.*, 2013, **46**, 1053–61.
11. I. Hung, L. Zhou, F. Pourpoint, C. P. Grey, and Z. Gan, *J. Am. Chem. Soc.*, 2012, **134**, 1898–901.
12. S. J. Harris, A. Timmons, D. R. Baker, and C. Monroe, *Chem. Phys. Lett.*, 2010, **485**, 265–274.
13. O. Borodin, G. V. Zhuang, P. N. Ross, and K. Xu, *J. Phys. Chem. C*, 2013, **117**, 7433–7444.
14. O. Borodin and D. Bedrov, *J. Phys. Chem. C*, 2014, **118**, DOI: 140723165951001.
15. K. Xu, *Chem. Rev.*, 2004, **104**, 4303–417.
16. M. Nie, D. P. Abraham, D. M. Seo, Y. Chen, A. Bose, and B. L. Lucht, *J. Phys. Chem. C*, 2013, **117**, 25381–25389.
17. A. von Cresce and K. Xu, *Electrochem. Solid-State Lett.*, 2011, **14**, A154.
18. K. Xu, Y. Lam, S. S. Zhang, T. R. Jow, and T. B. Curtis, *J. Phys. Chem. C*, 2007, **111**, 7411–7421.
19. S. J. Harris and P. Lu, *J. Phys. Chem. C*, 2013, **117**, 6481–6492.
20. K. Xu, A. von Cresce, and U. Lee, *Langmuir*, 2010, **26**, 11538–43.
21. K. Xu and A. von Wald Cresce, *J. Mater. Res.*, 2012, **27**, 2327–2341.
22. M. S. Ding, *J. Electrochem. Soc.*, 2004, **151**, A40.

23. L. Yang, A. Xiao, and B. L. Lucht, *J. Mol. Liq.*, 2010, **154**, 131–133.
24. V. P. Reddy, M. C. Smart, K. B. Chin, B. V. Ratnakumar, S. Surampudi, J. Hu, P. Yan, and G. K. Surya Prakash, *Electrochem. Solid-State Lett.*, 2005, **8**, A294.
25. M. Takeuchi, Y. Kameda, Y. Umebayashi, S. Ogawa, T. Sonoda, S. Ishiguro, M. Fujita, and M. Sano, *J. Mol. Liq.*, 2009, **148**, 99–108.
26. C. M. Burba and R. Frech, *J. Phys. Chem. B*, 2005, **109**, 15161–4.
27. K. Kondo, M. Sano, and A. Hiwara, *J. Phys. Chem. B*, 2000, **104**, 5040–5044.
28. M. Morita, Y. Asai, N. Yoshimoto, and M. Ishikawa, *J. Chem. Soc., Faraday Trans.*, 1998, **94**, 3451–3456.
29. P. Ganesh, D. Jiang, and P. R. C. Kent, *J. Phys. Chem. B*, 2011, **115**, 3085–90.
30. S.-A. Hyodo and K. Okabayashi, *Electrochim. Acta*, 1989, **34**, 1551–1556.
31. J. L. Allen, O. Borodin, D. M. Seo, and W. a. Henderson, *J. Power Sources*, 2014, **267**, 821–830.
32. Y. Kameda, Y. Umebayashi, M. Takeuchi, M. A. Wahab, S. Fukuda, S. Ishiguro, M. Sasaki, Y. Amo, and T. Usuki, *J. Phys. Chem. B*, 2007, **111**, 6104–9.
33. X. Bogle, R. Vazquez, S. Greenbaum, A. von W. Cresce, and K. Xu, *J. Phys. Chem. Lett.*, 2013, **4**, 1664–1668.
34. M. Castriota, E. Cazzanelli, I. Nicotera, L. Coppola, C. Oliviero, and G. A. Ranieri, *J. Chem. Phys.*, 2003, **118**, 5537.
35. K. R. Wilson, B. S. Rude, J. Smith, C. Cappa, D. T. Co, R. D. Schaller, M. Larsson, T. Catalano, and R. J. Saykally, *Rev. Sci. Instrum.*, 2004, **75**, 725–736.
36. D. Prendergast and G. Galli, *Phys. Rev. Lett.*, 2006, **96**, 215502.
37. A. M. Duffin, A. H. England, C. P. Schwartz, J. S. Uejio, G. C. Dallinger, O. Shih, D. Prendergast, and R. J. Saykally, *Phys. Chem. Chem. Phys.*, 2011, **13**, 17077–83.
38. A. M. Duffin, C. P. Schwartz, A. H. England, J. S. Uejio, D. Prendergast, and R. J. Saykally, *J. Chem. Phys.*, 2011, **134**, 154503.
39. A. H. England, A. M. Duffin, C. P. Schwartz, J. S. Uejio, D. Prendergast, and R. J. Saykally, *Chem. Phys. Lett.*, 2011, **514**, 187–195.
40. O. Shih, A. H. England, G. C. Dallinger, J. W. Smith, K. C. Duffey, R. C. Cohen, D. Prendergast, and R. J. Saykally, *J. Chem. Phys.*, 2013, **139**, 035104.
41. K. R. Wilson, B. S. Rude, T. Catalano, R. D. Schaller, J. G. Tobin, D. T. Co, and R. J. Saykally, *J. Phys. Chem. B*, 2001, **105**, 3346–3349.
42. C. D. Cappa, J. D. Smith, K. R. Wilson, and R. J. Saykally, *J. Phys. Condens. Matter*, 2008, **20**, 205105.

43. O. Borodin, *J. Phys. Chem. B*, 2009, **113**, 11463–78.
44. A. von Wald Cresce, O. Borodin, and K. Xu, *J. Phys. Chem. C*, 2012, **116**, 26111–26117.
45. O. Borodin and G. D. Smith, *J. Phys. Chem. B*, 2009, **113**, 1763–76.
46. D. M. Seo, O. Borodin, S.-D. Han, P. D. Boyle, and W. A. Henderson, *J. Electrochem. Soc.*, 2012, **159**, A1489–A1500.
47. P. Giannozzi, S. Baroni, N. Bonini, M. Calandra, R. Car, C. Cavazzoni, D. Ceresoli, G. L. Chiarotti, M. Cococcioni, I. Dabo, A. Dal Corso, S. de Gironcoli, S. Fabris, G. Fratesi, R. Gebauer, U. Gerstmann, C. Gougoussis, A. Kokalj, M. Lazzeri, L. Martin-Samos, N. Marzari, F. Mauri, R. Mazzarello, S. Paolini, A. Pasquarello, L. Paulatto, C. Sbraccia, S. Scandolo, G. Sclauzero, A. P. Seitsonen, A. Smogunov, P. Umari, and R. M. Wentzcovitch, *J. Phys. Condens. Matter*, 2009, **21**, 395502.
48. J. P. Perdew, K. Burke, and M. Ernzerhof, *Phys. Rev. Lett.*, 1996, **77**, 3865–3868.
49. J. Stöhr, *NEXAFS Spectroscopy*, 1992, vol. 25.
50. C. P. Schwartz, J. S. Uejio, R. J. Saykally, and D. Prendergast, *J. Chem. Phys.*, 2009, **130**, 184109.
51. K. Momma and F. Izumi, *J. Appl. Crystallogr.*, 2008, **41**, 653–658.